

CONFERENCE PRE-PRINT

THE STATUS AND DESIGN CHALLENGES OF THE HEATING AND CURRENT DRIVE SYSTEMS FOR DTT

G.GRANUCCI

Institute for Plasma Science and Technology, National Research Council (ISTP-CNR),
Milano, Italy
and
DTT S.C.a r.l.
Frascati, Italy
Email: gustavo.granucci@dtc-project.it

S.CECCUZZI, A.ROMANO

ENEA, Fusion and Nuclear Safety Department
Frascati, Italy
and
DTT S.C.a r.l.
Frascati, Italy

G.L. RAVERA

ENEA, Fusion and Nuclear Safety Department
Frascati, Italy

P.AGOSTINETTI, A.MURARI, A.FERRO, M.RECCHIA

Consorzio RFX (CNR, ENEA, INFN, University of Padova, Acciaierie Venete SpA)
Padova, Italy
and
Institute for Plasma Science and Technology, National Research Council (ISTP-CNR)
Padova, Italy

A.BRUSCHI F.FANALE, S.GARAVAGLIA, A.MORO¹ N.RISPOLI

Institute for Plasma Science and Technology, National Research Council (ISTP-CNR),
Milano, Italy

A.CIOFFI and DTT contributors

DTT S.c.a r.l.
Frascati, Italy

A.PEPATO

National Institute for Nuclear Physics (INFN)
Padova, Italy

C.SALVIA

University of Padua
Padova, Italy

A.A.TUCCILLO

CREATE
Napoli, Italy

Abstract

This paper reports the main design keys and the challenging issues of the Heating and Current Drive System (HCD) of the Divert Tokamak Test (DTT) facility that is under construction at ENEA site in Frascati with the aim to perform studies on the power exhaust in a flexible and easily modifiable environment. The selected HCD systems for DTT are those with the more consolidated technology and expected to be relevant for the future reactor. The status of each system is reported, both in terms of design and procurement, which are well advanced for the system required in the first phase of the DTT exploitation: electron and ion cyclotron resonant heating. The third system is neutral beam injector, based on negative ion acceleration, that will be installed in DTT in a second phase, after the first five years of operation. The full heating power will be reached with

the doubling of the radiofrequency power to reach the 45 MW at plasma needed to test the divertor with a power density at reactor level.

1. INTRODUCTION

The goal of the Divertor Tokamak Test facility (DTT) [1] is to perform power exhaust studies in reactor relevant conditions typical of ITER and DEMO, therefore its Heating and Current Drive (HCD) systems have been designed to load the divertor with a relevant power of 45 MW. The heating systems chosen for DTT are Electron Cyclotron (ECH - 32 MW at 170 GHz), Ion Cyclotron (ICH - 8 MW at 60-90 MHz) and negative Neutral Beam Injection (NBI - 10 MW at 510 keV). The DTT design is characterized by a large flexibility in the magnetic configurations, with the capability of investigating Single Null, X-Divertor, Double Null and Negative Triangularity, to allow the assessment of different divertor solutions. A large flexibility is also required for the design of the DTT plasma heating systems, to sustain the needed performances in all the operational conditions. DTT is a complex experiment and the integration challenges play a critical role in the design and development of the heating systems, providing, in turn, specific constraints to other auxiliary system like water cooling system, electrical power grid and the buildings for the HCD systems. The HCD power will be installed in 3 consecutive steps, in accordance with the DTT exploitation program: a first step with the installation of 16 MW of ECH and 4 MW of ICH, a second step with the addition of the 10 MW of NBI and the last one with the completion of the radio-frequency RF systems with further 16 MW for ECH and 4 MW for ICH. The duration of each step is presently foreseen to be approximately 5 years.

To support all the possible plasma configurations, that are expected to be used in DTT, movable antennas for the RF heating system and a certain degree of flexibility in the beam energy for NBI are required. This last capability has been included in the design requiring a step of at least 200 kV in the power supply of the accelerating grids allowing to operate the beam also in a relatively low-density plasma or during the current ramp up/down phases. A movable ICH antenna has been designed to maintain a good level of coupling also in case of plasma shape with large gap between separatrix and antenna box, that requires a cantilever design with the antenna weight sustained by external railways and an external driving system to move it in the required position. The several tasks assigned to ECH system impose a front steering solution for the launcher, with the capability to move poloidally and toroidally the individual launching mirror, aiming to possible different tasks at the same time (i.e. central heating and MHD stabilization) maintaining the maximum flexibility.

The relatively small dimensions and the high energy stored in the DTT plasma represent a further severe challenge for antennas with movable item facing the plasma, due to the mechanical constraints for the thermal loads and the forces induced by disruptions. The power load from plasma is assumed to be 0.5 MWm^{-2} to be added to the specific load due to the transmitted power, this requires an accurate design of the cooling of all the component facing the plasma. The second challenge is represented by the forces induced by disruption. To evaluate the relevance that these forces can have in DTT, one can compare the parameters that play the main role in determine the intensity of such forces: plasma current, local toroidal field and disruption time. In Table 1 a comparison of main tokamak is reported. The induced forces during disruption can be considered proportional to the following expression:

$$I_p \frac{B_0 R_0}{R_0 + a} \frac{1}{a^2}$$

where the second term consider the toroidal field at the outer equatorial plane (the part of the antennas close to plasma) and the last one is the dependency of disruption speed (proportional to the plasma cross-section).

TABLE 1. INDICATIVE COMPARISON OF E.M. LOAD OF DIFFERENT TOKAMAKS

	$B_0(\text{T})$	$I_p (\text{MA})$	$R_0(\text{m})$	$a(\text{m})$	$I_p \frac{B_0 R_0}{R_0 + a} \frac{1}{a^2}$
JET	3.4	5	2.96	1.25	7.6
AUG	3.2	1.4	1.65	0.5	13.7
JT60SA	2.25	5.5	2.96	1.18	6.3
EAST	3.5	1	1.85	0.45	13.9
KSTAR	3.5	2	1.8	0.5	21.9
ITER	5.3	15	6.2	2	15

DTT	5.85	5.5	2.19	0.7	49.7
-----	------	-----	------	-----	------

Due to its compactness and high field and plasma current, DTT is well above the level of electromagnetic loads in other tokamaks. This has required a proper and robust mechanical design of all movable part, with the exclusion of materials with high electrical conductivity (like CuCrZr for ECH last mirrors) or to set higher limits for tensile yield strength for the allowable materials. A further strong constrain is the pulse length of DTT (100 s) that requires an accurate cooling of all components transmitting high power to plasma.

2. THE ECH SYSTEM

The ECH system [2] is foreseen to support several functional tasks for plasma heating and control. The total power of the DTT ECH system, 32 MW installed, requires many equipment to be integrated in a compact layout and a challenging design of the antennas, 8 in total and located in 4 different sectors, to manage the high power density by maintaining a good flexibility to cover the different tasks. A modular scheme for a total of 4 clusters has been implemented, each of them composed by 8 gyrotrons with the related beams collected to a single quasi optical multibeam transmission line at the end of which the 8 beams are then split and injected separately in the plasma with independent launchers, steerable in the two directions. Table 2 reports the main functional parameters and characteristics of the DTT ECH system.

TABLE 2. MAIN FUNCTIONAL PARAMETERS OF THE DTT ECH

Parameter	Value
Frequency/Unit Power	170 GHz / 1 MW
Installed Power / Transmission Efficiency	32 MW / >90%
Plasma relative minor radius coverage	0-0.8 equatorial, 0.2-0.85 upper
Toroidal Injection angle	$\pm 25^\circ$ equatorial, $\pm 22.5^\circ$ upper
Steering speed	20°/s, $\Delta p/dt = 0.6/s$
Beam radii	44.5 mm equatorial, 27 mm upper
Power modulation	100% up to 5 kHz

In the first DTT phase, 2 clusters will be realized and installed for a power of 16 MW. The procurement of 16 RF sources is started and the gyrotrons are under manufacturing by THALES AVS France. A first pre-series unit has been tested up to the required performances at FALCON test facility (Fig. 1a), Swiss Plasma Centre in Lausanne (Switzerland). The results are shown in Fig. 1b, where 0,99 MW have been measured after the Matching Optics Unit during a 100 s pulse test, with an RF power stable within 5%, a current beam of 48 A in average and an acceleration voltage of 79.5 kV. The present schedule foresees the completion of the first 8 gyrotron delivery within 2028 to be installed and commissioned on-site, then ready for the first DTT plasma.

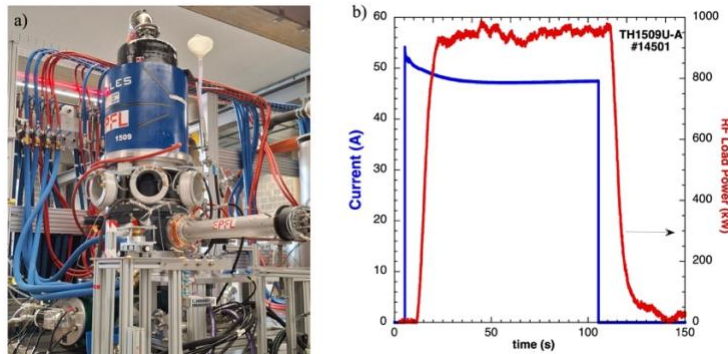


FIG. 1. a) First DTT gyrotron at FALCON test facility for commissioning and test b) Time evolution of the thermal power measurement (red) and related beam current (blue) for #14501 FALCON pulse.

Two gyrotrons will share a single high voltage Power Supply (PS) set feeding the cathodes, the body electrode and the filament heaters, and for which the conceptual design (similar to those done for ITER) has been completed and the technical specifications defined to start procurement of the eight sets needed [3]. The main PS

drives the electron beam (-60 kV, 110A), while the body PS is dedicated to the beam acceleration (30 kV, 100 mA), together allowing a 100% power modulation up to 5 kHz.

The conceptual design of the quasi-optical transmission line [4] has been completed (at least 80 mirrors over about a 100 m length to transport the RF power of each cluster) and a prototyping activity on mirrors has been started, exploiting the additive manufacturing technique to realize optimized cooling circuits capable to sustain and manage the highly localized thermal load minimizing also the surface deformations. Spiral cooling channel has been selected for each mirror type, both for the Single Beam (SB) mirror and for the Multi Beam (MB) mirrors to simplify water monitoring. The present design ensures deformations of about 30 μm for the SB mirrors including the combiner (Fig.2a) which is subject to a thermal load 6 times higher than the other SB mirror. Regarding the MB mirrors the thermo-mechanical analysis is under finalization, with a target of maximum deformation below 80 μm . The resulting deformed surfaces will be used to update the transmission line performances by calculation with the GRASP code, to compare them with those found in ideal case ($\sim 6.5\%$ for the first two clusters).

An evacuated compact connection line to direct the gyrotron output to the RF load, also designed to host different mirror's prototype, has been realized to be used in FALCON test facility, with the DTT first gyrotron, to validate mirrors design and manufacturing techniques. The realization of the 4 RF loads needed for the first 2 clusters is on-going to be completed in 2026 by Curti Costruzioni Meccaniche-LT Calcoli. One of the RF load in the cluster, in the gyrotron hall, is dedicated to daily conditioning of the gyrotrons, and a second one, at the end of MB transmission line, for mirrors conditioning, diagnostics calibration, alignment and polarization verification.

The ECH antenna has been designed assuring the maximum flexibility in terms of poloidal and toroidal launch angles. Each antenna integrates a dedicated quasi-optical launcher for each beam, 6 and 2 respectively in the equatorial and upper antenna, each one composed by 2 mirrors: a fixed focusing mirror and a steerable flat mirror, allowing precise and independently adjustment of the beam direction. The challenge in design is to face the paramount forces induced by major disruptions of DTT, as discussed in Section1.

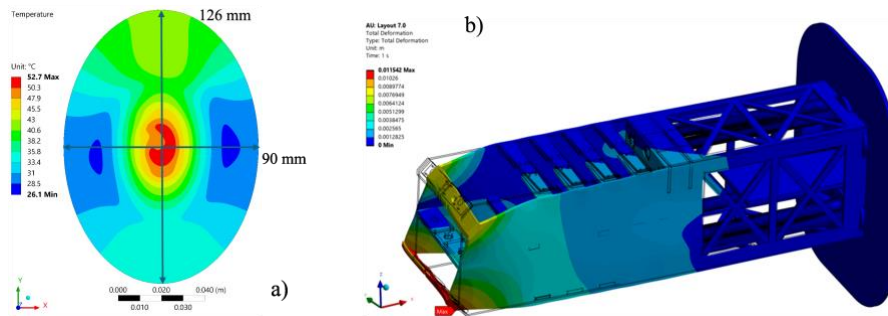


FIG. 2. a) Thermal field for combiner mirror. b) Total displacement of the equatorial antenna structure in case of a VDE.

The launchers supporting structures have been optimized after an electromagnetic analysis, to determine the forces, moment reactions and the consequent maximum displacement, under the electromagnetic loads generated during a vertical disruption event (VDE) scenario, taken as a worst case. Fig.2b shows the equatorial antenna where the total deformation is maximum 11.5 mm on the bottom part. A revision of the structure introducing insulation to limit current loops, helps in reducing maximum deformation below 10 mm on the whole system. In parallel, launching mirrors are under study to achieve efficient cooling with minimal surface deformation and stress under high thermal loads and to reduce induced currents during plasma disruptions. The requirements are conflicting, because effective cooling demands high-thermal conductivity materials like copper alloys, whereas minimizing induced currents calls for materials with low electrical conductivity. A composite material is under consideration with a strong Nickel alloy as possible alternative.

The selection of the in-vessel steering mechanism for the launching mirrors will be made between two potential solutions, one based on piezoelectric walking drive and the other on electro-hydraulic actuation, comparing feasibility and capability to enhance dynamic performance, ensuring a lifetime compatible with DTT project and its operational plan (up to 25000 pulses). The final choice of the driving system and mirrors materials will be addressed at the end of a prototyping activities.

3. ICH SYSTEM

The DTT ICH system [5] is composed by two modules, each of them based on 4 RF generators (transmitters), realized with Solid-State Power Amplifiers, connected by a transmission line and matching units to two movable 3-strap antennas. The antenna has been designed to guarantee efficient coupling in the single-null (SN) scenario of DTT and deliver power on a best-effort basis in the other foreseen magnetic configurations. The realization of 2 of the 4 transmitters of the first module of ICH system is ongoing and is expected to be completed by 2026. Together with the transmitter a batch of RF components, needed to realize a testbed for the transmitter test, has been procured with components, as the 2.5 MW RF load, to be used also in the final installation.

TABLE 3. MAIN FUNCTIONAL PARAMETERS OF THE DTT ICH MODULE

Parameter	Value
Frequency Rang	60-90 MHz
Installed Power	4.8 MW
Pulse Length	50 s
Max available CW power	480 kW
Power to SN plasma	≥ 3 MW
Antenna Power Density	$< 3\text{MW/m}^2$

The ICH system is designed to operate in the range 60-90 MHz as requested by the research program of DTT, allowing minority heating schemes in Hydrogen or in ^3He (see FIG 3).

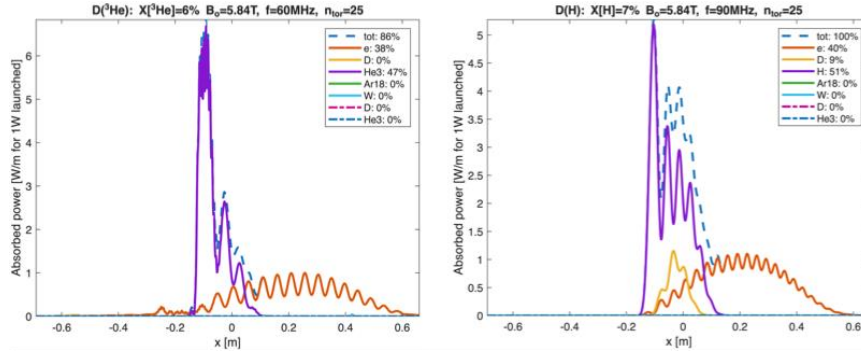


FIG 3. Single-pass absorption by plasma species vs. minor radius, predicted by TOMCAT [6] with ^3He minority at 60 MHz (left) and with H minority at 90 MHz (right) for the toroidal wave number maximally excited by the ICH antenna.

Main system capabilities are summarized in Table 3. Each ICH module is expected to couple 3 MW to the DTT reference plasma scenario for 50 s every hour while during wall conditioning operations, a larger duty cycle of 1 hour every 2 hours with a maximum coupled power of 200 kW was instead assumed. Each transmitter will consist of 128 RF modules that have been conceived with the robust design reliability used in broadcasting transmitters to sustain the reflection issue typical of plasma ICH coupling. A gradual, multi-stage, combination strategy has been designed, optimizing the performance at the edges of the frequency range, where the transmitters are mostly expected to operate. The transmitter outputs are combined in pairs and, after around 60 m of coaxial line, again split by 3 dB hybrid couplers and routed toward different antennas to feed equivalent straps. Each 3-strap antenna has 4 feeds, two for the central strap and the other two are for lateral ones (see FIG. 4).

Taking into account all geometrical constraints, the antenna design was optimized in terms of RF performance reaching a coupling capability in single null scenario well above the target value of 1.5 MW, pursuing the minimization of parallel RF near fields, which are widely consider a major cause of enhanced sputtering during ICH operations (see FIG. 5). To keep at a reliable level of power density, the antenna requires a space larger than the port area, forcing to install it from inside by remote handling. Therefore, the current design is based on a “semi plug-in” concept, where straps and most part of antenna box are installed through the port whereas the remaining components like Faraday screen and limiters will be assembled by the Remote Handling System.

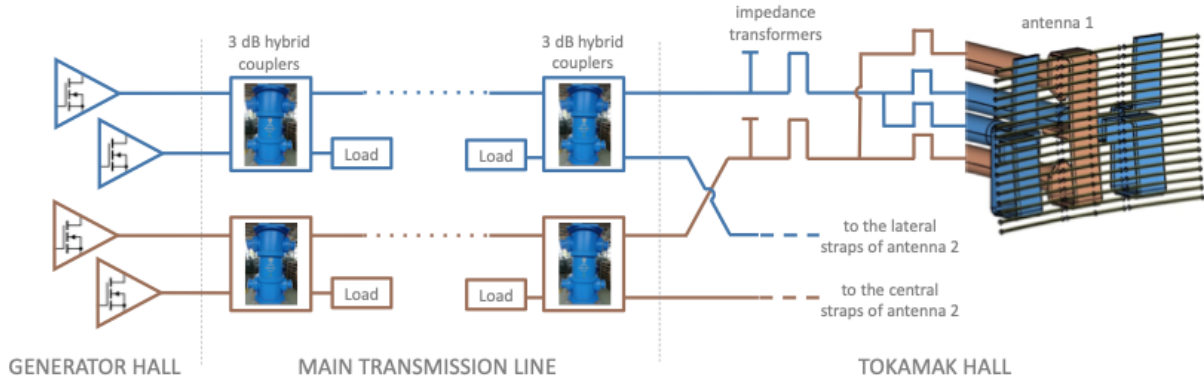


FIG. 4. Circuit diagram of the transmission line of the ICH system of DTT.

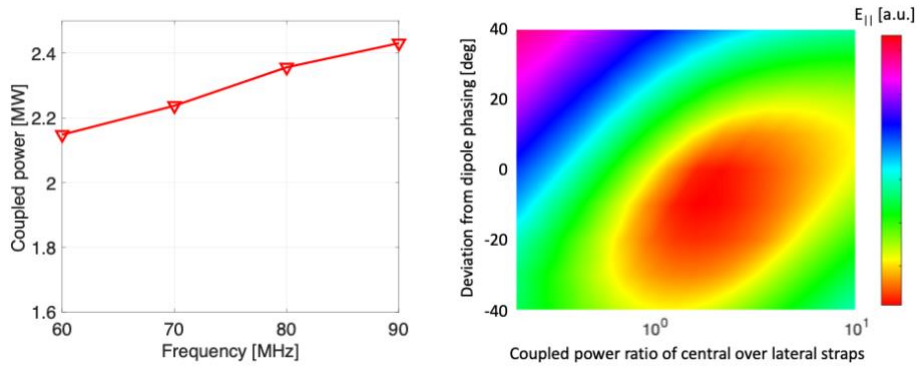


FIG. 5. (Left) Power coupling capability of the ICH curved antenna model, calculated with TOPICA [7] assuming dipole phasing, a maximum voltage of 35 kV in the coaxial feeds, and same coupled power between central and lateral straps. (Right) Parallel radiofrequency electric field averaged 3 mm in front of an antenna side limiter vs. power and phase unbalances between central and lateral straps, calculated with TOPICA under a flat antenna approximation at 90 MHz.

4. NBI SYSTEM

The DTT NBI system [8] will be installed for the second phase of the scientific program. The conceptual design has been completed. Starting from the prototypes for ITER, SPIDER and MITICA, some specific optimization has been done to adapt it to the DTT requirements. An overview of its conceptual design is given in FIG. 6, while Table 4 reports the main functional parameters.

A design with an air-insulated beam source has been adopted for DTT NBI, i.e. the accelerator and ion source assemblies are connected to the rear part of the vacuum vessel, as shown in Fig. 1a. This solution has been selected because it maximizes the Reliability and Availability indexes (evaluated as in [9]). The DTT NBI will feature the same Radio Frequency source concept chosen for ITER, under test in NBTF. The Beam Line Components (BLC), i.e. the Neutralizer, the Residual Ion Dump (RID) and the Calorimeter, will be also ITER-like. For the vacuum pumping, it is foreseen to have a system based on turbo-molecular pumps located on the side walls of the vessel and Non-Evaporable Getter pumps located on the upper and lower surfaces of the vessel.

Small flanges are foreseen on the vacuum vessel for pumping, diagnostics and BLCs supplies, while the maintenance is planned to be executed from the large circular flange of the accelerator, after removing the ion source and accelerator itself. Dedicated rails are hosted inside the vacuum vessel to insert and extract the BLCs, and to support them when they are in position. The maintenance of the ion source and accelerator will be performed using a dedicated maintenance platform, able to reach the critical regions of these components.

A HV transmission line and a cooling tower are located at the two sides of the ion source. The first brings the electrical power to the ion source and accelerator by means of a high voltage bushing connecting the grounded transmission line to the ion source and to two acceleration grids. The second tower connects the cooling water to

the ion source and to the accelerator. Also the piping for the deuterium inlet and the exhaust of the high voltage vacuum system will pass through the cooling tower, as they are also connecting to ground high voltage components (-510 kV).

TABLE 4. MAIN FUNCTIONAL PARAMETERS OF THE DTT NBI

Parameter	Value
Injected Power	10 MW
Beam Energy	510 keV
Accelerated D^0 Current	40 A
Extracted D^- Current Density	$> 239 \text{ Am}^{-2}$
Pulse length	50 s
Overall Efficiency	0.357
Beamlet divergence	$> 7 \text{ mrad}$

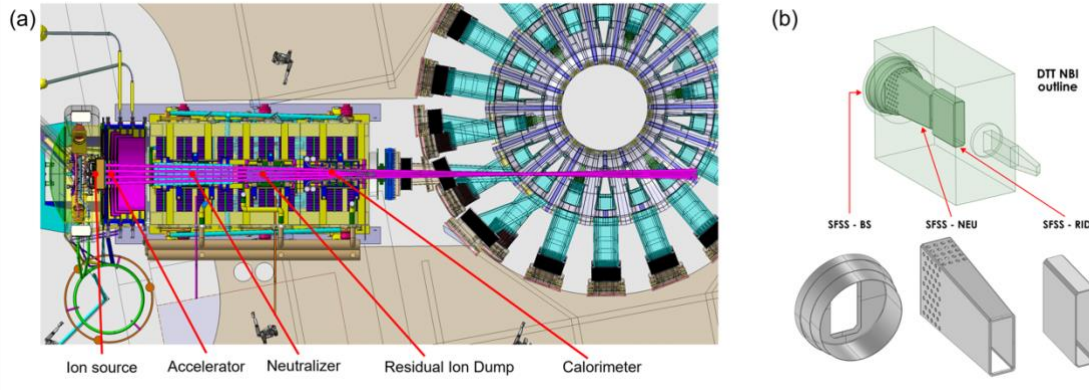


FIG. 6. Left- Top view of the DTT NBI conceptual design with beamline component indication. Right- Scheme of the Stray Field Shielding System for DTT NBI, in grey the ferromagnetic element composing it.

Due to the small distance with the tokamak, the NBI injector is interested by a relevant stray vertical field, that could reduce the overall efficiency of the NBI system and increasing the heat loads on the main components. To avoid this effect a Stray Field Shielding System (SFSS) made of ferromagnetic material has been developed.

The SFSS, whose conceptual design is shown in Fig. 6 -right, features three sections: a section on the beam source (SFSS - BS) to protect the beam from unwanted deflections in the accelerator; a section on the neutralizer (SFSS - NEU) to avoid deflections of the negative ions in the neutralizer and finally a section on the RID (SFSS - RID) to avoid charged particles to escape from the RID. The introduction of this version of SFSS allows the efficiency of the NBI can be kept at high values (as reported in Tab. 4) also in presence of the high stray fields generated by the tokamak. The port duct connects the injector to the Tokamak, allowing the neutral beam to reach the plasma, providing the required ion heating and current drive. In the port duct, a fraction of the high-energy neutral particles (D^0) is transformed into positive ions (D^+) by re-ionization reactions due to the presence of background gas. These highly energetic D^+ ions are then deflected by the local magnetic fields becoming concentrated heat loads on the internal surfaces of the duct, with peak power density in the order of 3 MW m^{-2} . To protect it, a duct liner has been designed, made of CuCrZr and actively cooled. A double cooling spiral design has been adopted, to increase the tubes density on the region where the heat load is expected to be maximum. Simulations show that the temperature of the point interested by the peak loads are below critical values for the material used.

The NBI acceleration system will be manufactured adopting the Additive Manufacturing (L-PBF: laser powder bed fusion) for metals technology, both for the accelerating grids and for the suspension system. The insulating metallic rings will be manufactured by means of the composite material technology, while the metallic rings with the more standard subtractive technology. The advantages of L-PBF technology process, in terms of material properties, optimization design and innovative cooling layout are exploited in the design of the grids [10]. The reference material is the CuCrZr alloy for its mechanical properties, despite a small variation of the thermal conductivity with respect to copper: 309 W/m K instead of 370 W/m K of Cu. The high surface roughness,

obtained using LPBF technology, can be removed with conventional milling but can affect the pressure drop in cooling channels which could be an important limiting factor.

The implementation of the LPBF technology led to some relevant modifications: the concept design has been changed, and the whole design of the grids has been modifying slightly the beam optics components and completely the cooling circuit, as reported in Fig. 7-left. To better focus the ion beam the shape of the grids is spherical. This design improves also the overall rigidity.

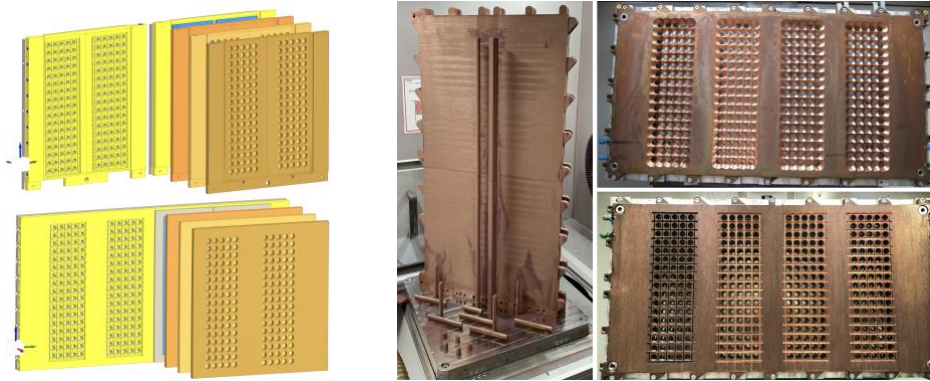


FIG. 7. Left: Grid's design modifications: the traditional subtractive approach (left top) and the spherical one made with AM (left bottom). Right: Full-size Plasma & Extraction grids raw blanks (left); full-size finished Plasma Grid (front: right top) and finished Extraction Grid (front: right bottom).

Due to the dimensions of the entire grid plane (1760x840mm) and the physical limitations of the 3D printing machines, for manufacturing purposes, the grid has been divided into 4 elements of 440x840mm. After a first prototype (5x17 beamlets, 440 x 210mm), produced by EOS-Turku and machined by INFN-PD, two full-scale prototypes of plasma and extraction grid (4x5x17 beam-lets, 440x840mm) have been produced. These prototypes (see Fig.7 right) will be used to set the production process, to establish an alignment protocol and to perform first experimental tests. The R&D program on additive manufacturing for metals implementation performed at DIAM INFN PD demonstrates that this technology offers extremely good opportunities with consistent reduction on costs, production time, and morphological improvements for complex geometries.

The Acceleration Grid Power Supply of the NBI is rated -500 kV dc (divided in 3 stages), ~70 A. The feasibility of a solution based on a double conversion stage with ac/dc rectifier, dc-link, dc/ac inverters, step-up transformers and HV gas-insulated diode rectifiers, has been preliminarily verified [11]. In parallel, the feasibility of a solution based on Modular Multilevel Converters (MMC) has been explored. It would provide advantages as lower energy transferred during the grid breakdowns, much less gas-insulated components and low voltage ripple. On the other hand, the MMC needs very large building for insulation and maintenance. Therefore, to finally assess the feasibility of the MMC technology for this application and for the DTT site, a preliminary engineering design should be done in collaboration with industry.

REFERENCES

- [1] F. ROMANELLI, Nucl. Fusion **64** (2024) 112015
- [2] G. GARAVAGLIA et al., J. of Vac. Sci. Tech. B **41** (2023) 044201
- [3] M. RECCHIA et al., IEEE Tran. Plasma Scie., **52** (2024) 4069-4074
- [4] F. FANALE et al., IEEE Tran. Plasma Scie **52** (2024) 3778-3784.
- [5] S. CECCUZZI - et al, Fusion Eng. and Des. **213** (2025), 114849
- [6] D. VAN EESTER et al., Plasma Phys. Control Fusion **40** (1998) 1949-1975
- [7] V. LANCELLOTTI et al., Nucl. Fusion **46** (2006) S476–S499
- [8] P. AGOSTINETTI et al. IEEE Tran. Plasma Scie., **50** (2022) 4027-4032
- [9] P. AGOSTINETTI, et al., Fusion Eng. and Des., **159** (2020) 111628
- [10] A. PEPATO et al., Fusion Eng. Des. **219** (2025) 115238
- [11] A. FERRO et al., Fusion Eng. Des. **169** (2021) 11262